NONLINEAR ANALYSIS OF BONDED COMPOSITE PATCH REPAIRS

Quantian Luo, Liyong Tong
School of Aerospace, Mechanical and Mechatronic Engineering, The University of Sydney, NSW 2006, Australia

Keywords: *nonlinear analysis, adhesive bonding repair, cracked structure*

Abstract

This paper presents a geometrical nonlinear analysis for the single strap model of single-sided adhesively bonded composite patch repairs to cracked structures subjected to tension. In this analysis, the equilibrium equations are derived by considering the large deflections of the substrates along their entire lengths. By neglecting the higher order items, analytical solutions for the single-strap patch repair model are obtained, and the solutions are then simplified for engineering applications. The geometrically-nonlinear finite element analysis was conducted using MSC/NASTRAN to validate the present closed-form solutions. The numerical results indicate that the present closed-form solutions and their simplifications correlate very well with the nonlinear finite element computations.

1 Introduction

Adhesively bonded patch repair technology has been widely used to extend the service life of a cracked structure. It is easy to use in practice and can significantly enhance structural performance. To efficiently apply this technology, stress analysis for this type of bonding structure must be conducted [1]-[2]. In practice, bonded composite patch repairs can come in two forms: double-sided patches and single-sided patch. The single-sided patch repair has been most widely used because it is practically easy to access one side of a cracked structure.

Figure 1 depicts a simple single-strap joint model studied here for simulating a strip of a single-sided patch repair to a cracked structure. When there is no support in the overlap region, large out-of-plane deflections in both substrates have been observed [3]-[4]. In this case, it is difficult to obtain analytical solutions for such a single-strap joint due to geometrical nonlinearity. Thus geometrical nonlinear finite element analysis (NFEA) has been widely used to take into account the large deflections and to predict stresses in adhesive and substrates [5]-[8].

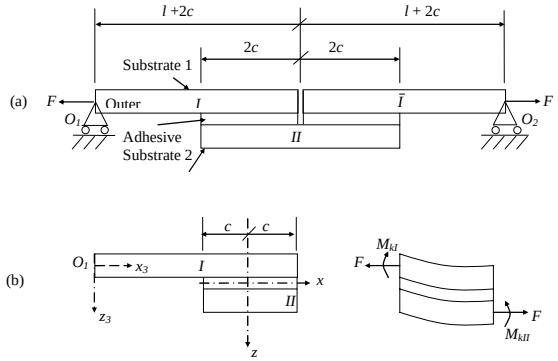

Fig. 1 A single strap joint model for simulating single-side patch repair

To develop closed-form solutions for the single-strap joint shown in Fig. 1, it is important to review the works done for single-lap joints. In 1944, Goland and Reissner [9] presented a stress analysis for adhesive joints. In determining the edge moment for the single lap joint, the overlap was treated as one single beam by ignoring the adhesive layer. In 1973, Hart-Smith attempted to extend the formulation given by Goland and Reissner by considering the influence of adhesive layer on the edge moment factor. However, the features of large deflections of the substrates were not included in his formulation [10]. Oplinger [11] attempted to include the influence of large deflections of the substrates in the Hart-Smith's formulation. In his formulation, only adhesive shear strain and substrate deflections were coupled based on the assumptions used in his paper. Recently we presented new closed-form solutions for nonlinear analysis of adhesively bonded single lap joints, in which large deflections

of the substrates in the overlap region are coupled with both adhesive strains [12]. In this paper, we intend to extend our solutions for single-lap joints to the case for single-strap joint as shown in Fig 1. To our best knowledge, there exist no such closed-form analytical solutions for a fully-coupled stress analysis of the adhesively bonded single-strap joint in Fig. 1 in the open literature.

2 Theoretical formulations and solutions

Consider the single-strap model shown in Fig 1, substrates 1 and 2 are assumed to be identical. They can be either isotropic or composite. For the case of composite substrates, the lay-up of each substrate is assumed to be symmetrical. To analyze this model, we subdivide the structure into 4 parts. Because of the symmetry, only the left half (Parts O_1-I and I_II) is considered.

2.1 Equilibrium equations

To develop the governing equations, the following variables are introduced:

$$\begin{cases} 2u_s = u_2 + u_1;\ 2w_s = w_2 - w_1;\ 2\phi_s = \phi_2 - \phi \\ 2u_a = u_2 - u_1;\ 2w_a = w_2 + w_1;\ 2\phi_a = \phi_2 + \phi_1 \\ 2N_s = N_2 + N_1; 2N_a = N_2 - N_1 \\ 2Q_s = Q_2 - Q_1;\ 2Q_a = Q_2 + Q_1 \\ 2M_s = M_2 - M_1;\ 2M_a = M_2 + M_1 \end{cases} \quad (1)$$

where u, w and ϕ are the axial displacement, transverse deflection and the angle of rotation, respectively; and N, M and Q are the stress resultants, as shown in Fig 2. The subscripts 1 and 2 denote the quantities for substrates 1 and 2 respectively, and s and a represent the symmetrical and anti-symmetrical combinations of these physical quantities.

The equilibrium equations considering large deflections of the substrates for the free body diagram shown in Fig.2 are:

$$\begin{cases} \dfrac{dN_1}{dx} + \tau = 0 \quad \dfrac{dQ_1}{dx} + \sigma + \tau\phi_1 = 0; \\ \dfrac{dM_1}{dx} + \dfrac{t_1}{2}\tau - Q_1 = -N_1\phi \\ \dfrac{dN_2}{dx} - \tau = 0 \quad \dfrac{dQ_2}{dx} - \sigma - \tau\phi_2 = 0 \\ \dfrac{dM_2}{dx} + \dfrac{t_1}{2}\tau - Q_2 = -N_2\phi_2 \end{cases} \quad (2)$$

where t_1 is the substrate thickness; τ and σ are the adhesive shear and peel stresses.

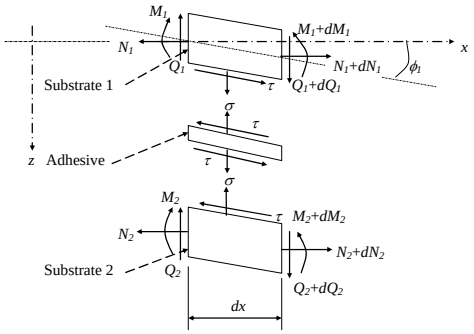

Fig. 2 Typical free body diagram in the overlap regions

By using the variables defined in Equation (1), the equilibrium equations can be transformed into:

$$\begin{cases} \dfrac{dN_s}{dx} = 0 \qquad \dfrac{dQ_s}{dx} - \sigma - \tau\phi_a = 0 \\ \dfrac{dM_s}{dx} - Q_s = -N_s\phi_s - N_a\phi_a \\ \dfrac{dN_a}{dx} - \tau = 0 \quad \dfrac{dQ_a}{dx} - \tau\phi_s = 0 \\ \dfrac{dM_a}{dx} + \dfrac{t_1}{2}\tau - Q_a = -N_s\phi_a - N_a\phi_s \end{cases} \quad (3)$$

In Equation (3), by differentiating the 3rd and 6th equations, into which substituting relations of the 1st, 2nd, 4th and 5th equations, and by neglecting the higher order items, we have:

$$\frac{dN_s}{dx} = 0;\ \frac{d^2M_s}{dx^2} - \sigma = -N_s\frac{d\phi_s}{dx} \quad (4)$$

$$\frac{dN_a}{dx} - \tau = 0;\ \frac{d^2M_a}{dx^2} + \frac{t_1}{2}\frac{d\tau}{dx} = -N_s\frac{d\phi_a}{dx} \quad (5)$$

Equations (4) and (5) are derived from a geometrically-nonlinear analysis for adhesive joints with the same thickness substrates. There is no other limitations except for neglecting the higher order items, $(u_a'\phi_s')$ and $(u_a'\phi_a')$.

It is noted that N_s is a constant, namely, $N_s = \frac{1}{2}F$, for the case considered in Fig 1 where the remote tensile force F is applied at the ends of the single-strap joint as a given constant.

2.2 Constitutive relationships

When identical substrates are considered and the Euler beam theory is employed, the constitutive relationships of the substrates and adhesive are [12]:

$$N_i = A_{11}\frac{du_i}{dx};\ M_i = -D_{11}\frac{d^2w_i}{dx^2}\ (i = s, a) \tag{6}$$

$$\tau = \frac{2G_a}{t_a}\left(u_a + \frac{t_1}{2}\frac{dw_a}{dx}\right);\ \sigma = \frac{2E_a w_s}{t_a} \tag{7}$$

in which, E_a and G_a are Young's and shear moduli of the adhesive; and t_a is the adhesive thickness.

2.3 Governing differential equations with large deflections

By combining equations (4)-(7), the governing differential equations for the single-lap overlap regions with large deflections can be derived as follows:

$$\begin{cases} \dfrac{d^2u_s}{dx^2} = 0 \\ D_{11}\dfrac{d^4w_s}{dx^4} - \dfrac{F}{2}\dfrac{d^2w_s}{dx^2} + \dfrac{2E_a}{t_a}w_s = 0 \end{cases} \tag{8}$$

$$\begin{cases} A_{11}\dfrac{d^2u_a}{dx^2} - \dfrac{2G_a}{t_a}\left(u_a + \dfrac{t_1}{2}\dfrac{dw_a}{dx}\right) = 0 \\ -D_{11}\dfrac{d^4w_a}{dx^4} + \dfrac{G_a t_1}{t_a}\left(\dfrac{du_a}{dx} + \dfrac{t_1}{2}\dfrac{d^2w_a}{dx^2}\right) + \dfrac{F}{2}\dfrac{d^2w_a}{dx^2} = 0 \end{cases} \tag{9}$$

2.4 Analytical solutions for the overlap regions

The analytical solutions for equations (8) and (9) are given respectively by:

$$\begin{cases} u_s = A_{s1}x + A_{s2} \\ w_s = (B_{s1}\sinh\beta_{s1}x + B_{s2}\cosh\beta_{s1}x)\sin\beta_{s2} \\ \quad + (B_{s3}\sinh\beta_{s1}x + B_{s4}\cosh\beta_{s1}x)\cos\beta_{s2}x \end{cases} \tag{10}$$

$$\begin{cases} u_a = A_{a1}\sinh\beta_{a1}x + A_{a2}\cosh\beta_{a1}x \\ \quad + A_{a3}\sinh\beta_{a2}x + A_{a4}\cosh\beta_{a2}x + A_{a5} \\ w_a = B_{a1}\sinh\beta_{a1}x + B_{a2}\cosh\beta_{a1}x + B_{a3}\sinh\beta_{a2}x \\ \quad + B_{a4}\cosh\beta_{a1}x + B_{a5}x + B_{a6} \end{cases} \tag{11}$$

In equations (10) and (11), the eigenvalues are given by:

$$\begin{cases} \beta_{s1} = \sqrt{\beta_\sigma^2 + \dfrac{\beta_k^2}{8}};\ \beta_{s2} = \sqrt{\beta_\sigma^2 - \dfrac{\beta_k^2}{8}} \\ \beta_{a1}^2 = \dfrac{1}{2}\left[\alpha_a\beta_\tau^2 + \dfrac{\beta_k^2}{2} + \sqrt{\alpha_a^2\beta_\tau^4 + (\alpha_a - \dfrac{1}{2})\beta_\tau^2\beta_k^2 + \dfrac{\beta_k^4}{4}}\right] \\ \beta_{a2}^2 = \dfrac{1}{2}\left[\alpha_a\beta_\tau^2 + \dfrac{\beta_k^2}{2} - \sqrt{\alpha_a^2\beta_\tau^4 + (\alpha_a - \dfrac{1}{2})\beta_\tau^2\beta_k^2 + \dfrac{\beta_k^4}{4}}\right] \\ \beta_\sigma = \dfrac{\sqrt{2}}{2}\times\sqrt[4]{\dfrac{2E_a}{D_{11}t_a}};\ \beta_\tau = \sqrt{\dfrac{8G_a}{A_{11}t_a}} \end{cases} \tag{12}$$

where,

$$\alpha_a = \frac{1}{4}(1 + \alpha_k);\ \alpha_k = \frac{A_{11}t_1^2}{4D_{11}} \tag{13}$$

For laminated substrates, the coefficients α_a and α_k reflect the influence of their lay-ups. For the isotropic materials, $\alpha_a = 1$ and $\alpha_k = 3$.

2.5 Analytical solutions for single-strap joints

The integration constants of equations (10) and (11) can be determined by using the boundary and continuity conditions. For the single-strap joint in Fig 1, the stress-resultant boundary conditions are:

At the end of overlap $x = -c$:

$$\begin{cases} \dfrac{du_s}{dx} = \dfrac{F}{2A_{11}};\ \dfrac{d^2w_s}{dx^2} = \dfrac{M_{kI}}{2D_{11}};\ \dfrac{d^3w_s}{dx^3} = \dfrac{\beta_k^2}{2}\dfrac{dw_s}{dx} \\ \dfrac{du_a}{dx} = -\dfrac{F}{2A_{11}};\ \dfrac{d^2w_a}{dx^2} = -\dfrac{M_{kI}}{2D_{11}} \\ \dfrac{d^3w_a}{dx^3} - \dfrac{A_{11}t_1}{2D_{11}}\dfrac{d^2u_a}{dx^2} = \dfrac{\beta_k^2}{2}\dfrac{dw_a}{dx} \end{cases} \tag{14}$$

At the other end of the overlap $x = c$:

$$\begin{cases} \dfrac{du_s}{dx} = \dfrac{F}{2A_{11}};\ \dfrac{d^2w_s}{dx^2} = -\dfrac{M_{kII}}{2D_{11}};\ \dfrac{d^3w_s}{dx^3} = \dfrac{\beta_k^2}{2}\dfrac{dw_s}{dx} \\ \dfrac{du_a}{dx} = \dfrac{F}{2A_{11}};\ \dfrac{d^2w_a}{dx^2} = -\dfrac{M_{kII}}{2D_{11}} \\ \dfrac{d^3w_a}{dx^3} - \dfrac{A_{11}t_1}{2D_{11}}\dfrac{d^2u_a}{dx^2} = \dfrac{\beta_k^2}{2}\dfrac{dw_a}{dx} \end{cases} \tag{15}$$

In equations (14) and (15), M_{kI} and M_{kII} are the edge moments at cross-sections *I* and *II*, which are to be determined. In equations (10) and (11), there are only 12 independent integration constants. In equations (14) and (15), there are 9 independent boundary conditions. Thus five extra conditions are required to determine the 12 integration constants and the two edge moment factors.

It is noted in equations (14) and (15) that the shear force *Q* is perpendicular to axis x, which is different from the shear force *V* in the deformed beam cross section.

2.6 Edge moment factors and their simplifications

Similar to Ref [9], the axial displacement u_3 and the large deflection w_3 for substrate O_1I can be expressed as:

$$u_3 = \frac{F}{A_{11}} x_3 + u_{o1}; w_3 = -\frac{M_{kI} \sinh \beta_k x_3}{F \sinh \beta_k l} \tag{16}$$

where,

$$\beta_k = \sqrt{\frac{F}{D_{11}}} \tag{17}$$

and u_{o1} is a unknown integration constant. Together with the solutions in equations (10) and (11), we need six conditions to determine six unknowns. These six conditions are:

At cross-section *I*, we have the following three displacement continuity conditions:

$$u_3(l) = u_1(-c) \ ; \ \ w_3(l) = w_1(-c) \ ; \ \ w_3'(l) = w_1'(-c) \tag{18a}$$

At cross-section *II*, we have the following three symmetrical conditions:

$$\begin{aligned} &u_2(c) = 0; w_2'(c) = 0 \\ &M_{kII} = -F[(t_1 + t_a) + w_2(c)] \end{aligned} \tag{18b}$$

With the six conditions, we can develop the closed-form expression for the edge moment factors.

When the approximations used in the adhesively bonded single lap joints in Ref [12] and $\beta_{a1} \approx \alpha_a \beta_\tau >> \beta_{a2}$ are employed, and the solutions of edge moment factors can be simplified into:

$$\begin{cases} k_I = \dfrac{\Delta_b \Delta_{22}}{\Delta_{11}\Delta_{22} - \Delta_{12}\Delta_{21}} \\ k_{II} = -\dfrac{\Delta_b \Delta_{21}}{\Delta_{11}\Delta_{22} - \Delta_{12}\Delta_{21}} \end{cases} \tag{19}$$

where:

$$\begin{cases} \Delta_b = 1 + \dfrac{\beta_k^2 c^2}{8\alpha_a (1 + t_a / t_1)} \left[\dfrac{\beta_{a2} c \coth \beta_{a2} c - 1}{\beta_{a2}^2 c^2} - \dfrac{(\beta_{a1} c - 1)}{\beta_{a1}^2 c^2} \right] \\ \Delta_{11} = 1 - \dfrac{\beta_k^2}{8\alpha_a \beta_{a2}^2} \left(1 - \dfrac{2\beta_{a2} c}{\sinh 2\beta_{a2} c} \right) - \dfrac{\beta_k^2}{4\beta_\sigma^2} \\ \Delta_{12} = 1 - \dfrac{\beta_k^2}{8\alpha_a \beta_{a2}^2} \left(1 - \dfrac{2\beta_{a2} c}{\tanh 2\beta_{a2} c} \right) + \dfrac{\alpha_k \beta_k^2 c}{4\alpha_a \beta_{a1}} + \dfrac{\beta_k^2 c}{\beta_\sigma} \\ \Delta_{21} = \coth \beta_k l + \dfrac{\beta_k}{8\alpha_a} \left(\dfrac{\alpha_k}{\beta_{a1}} + \dfrac{\tanh \beta_{a2} c}{\beta_{a2}} \right) + \dfrac{\beta_k}{2\beta_\sigma} \\ \Delta_{22} = -\dfrac{\beta_k}{8\alpha_a} \left(\dfrac{\alpha_k}{\beta_{a1}} + \dfrac{\tanh \beta_{a2} c}{\beta_{a2}} \right) - \dfrac{\beta_k}{2\beta_\sigma} \\ \Delta_{22} = -\dfrac{\beta_k}{8\alpha_a} \left(\dfrac{\alpha_k}{\beta_{a1}} + \dfrac{\tanh \beta_{a2} c}{\beta_{a2}} \right) - \dfrac{\beta_k}{2\beta_\sigma} \end{cases} \tag{20}$$

In Equation (19), edge moment factors are defined as:

$$k_I = \frac{M_{kI}}{F(t_1 + t_a)}; \ k_{II} = -\frac{M_{kII}}{F(t_1 + t_a)} \tag{21}$$

3. Numerical results

The present formulation can be applied to patch repairs of cracked structures of isotropic and composite substrates with symmetrical lay-ups. In this paper, we only present numerical results for the isotropic substrates. We use the following geometrical sizes and materials properties:

The isotropic substrates: t_1 = 1.6 mm, t_a = 0.2 mm, c/t_1 = 8, l/c = 5, which represents the relatively-short overlap, The material properties::E_1 = 70 GPa, ν_1 = 0.3.

The adhesive material properties: E_a = 2.4 GPa, ν_a = 0.4.

To verify the present closed form formulation, the geometrically-nonlinear finite element analysis (NFEA) is conducted using the commercial finite element analysis (FEA) package MSC/NASTRAN. It is noted that all geometrically-nonlinear properties of the repairs can be modeled in the FEA package.

3.1 Edge Moment factors k_I and k_{II}

The edge moment factors k_I and k_{II} for the isotropic patch repairs predicted by the present formulation and the geometrically-nonlinear finite element analysis (NFEA) are plotted in Figs 3 and 4.

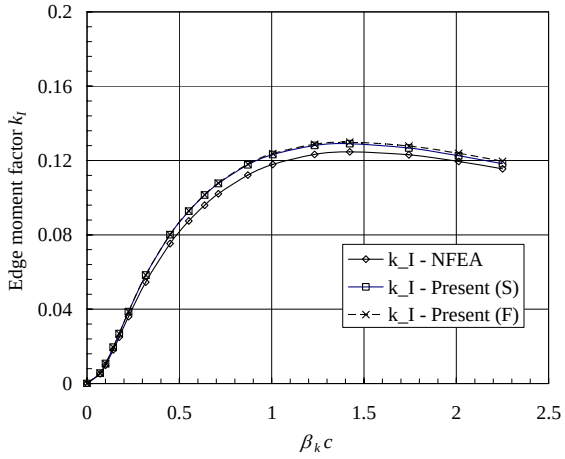

Fig.3 Edge moment factor k_I for the isotropic substrates

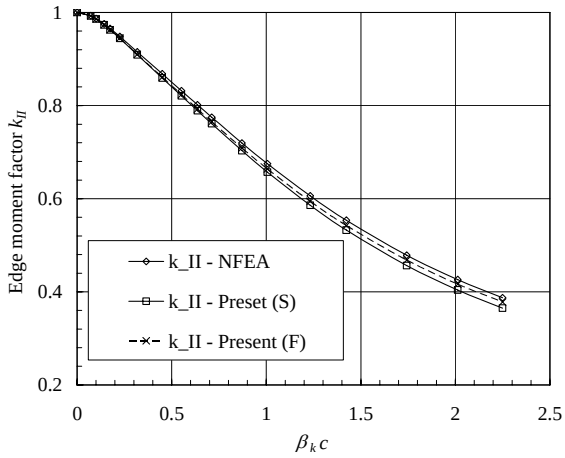

Fig.4 Edge moment factor k_{II}

Meanings of the abbreviations used in Figs 3 and 4 are: NFEA – geometrically-nonlinear finite element analysis, Present (S) – the present simplified solutions, and Present (F) – present full solutions. These abbreviations will always be used in Fig 5 of this paper.

It can be found from Fig 3 that, when $\beta_k c$ = 2.25, edge moment factors k_I present by the NFEA, the present simplified and full solutions are 0.115, 0.118 and 0.12 respectively. Fig 4 indicates that the corresponding values of edge moment factor k_{II} are 0.387, 0.365 and 0.378, respectively.

At $\beta_k c$ = 2.25, the axial average stress in the outer substrate O_1I is 507 MPa, which is normally larger than or close to the failure stress of a substrate. Thus it is reasonable to limit our numerical study to the case when $\beta_k c > 2.25$.

Figs 3 and 4 indicate that the present solutions for the edge moment factors k_I and k_{II} correlate with the present numerical results obtained using full geometrical nonlinear finite element analysis using MSC/NASTRAN. It also indicates that the present simplified solutions for both factors are in excellent agreement with their full solutions.

It is noted that k_I = 0 and k_{II} = 1 for the linear analysis of the single strap joint shown in Fig 1. This clearly shows the important role of the highly geometrical nonlinear property in predicting edge moment factors and then stresses in adhesive and substrates for the single-sided patch repairs as observed in Figs 3 and 4.

3.2 Influence of peel strain on the edge moment factors

In this section, we investigate the influence of peel strain on the edge moment factors. The contribution of the peel strain term may be neglected by directly ignoring the terms with subscript *s* in the solutions given by equations (19) and (20). Fig 5 depicts the computed k_I and k_{II} with and without considering the peel strain in the solution in equations (19) and (20).

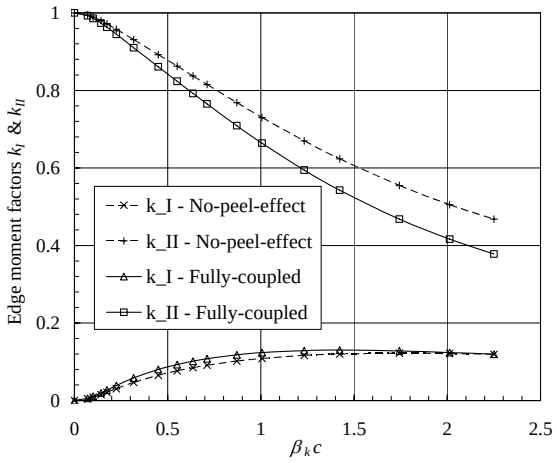

Fig.5 Edge moment factors with and without peel strain effect

Fig 5 indicates that, k_{II} = 0.378 and k_{II} = 0.468 for the fully coupled solution (namely with peel strain considered) and that without peel strain when $\beta_k c$ = 2.25. It is noted that ignoring the peel strain in the full solution leads to a 24% increase in the edge moment factor k_{II}. This shows that the peel strain must be included in the full coupled formulations.

4. Conclusion

This paper presented a geometrically-nonlinear analysis for the adhesively bonded single-strap joint. The derived analytical solutions and their simplifications for the single-sided composite patch repairs well correlate with the geometrically-nonlinear finite element analysis.

Numerical results demonstrated the highly-nonlinear property of the single-strap model for simulating the single-sided patch repairs. Fully-coupled formulation with large deflections of the overlap is generally required for analyzing the single-sided patch repairs of cracked structures.

Acknowledgement

The authors are grateful for the support of Australian Research Council via Discovery-Projects grant (DP0666683).

References

[1] Okafor A.C., Singh N., Enemuoh U.E. and Rao S.V., "Design, analysis and performance of adhesively bonded composite patch repair of cracked aluminum aircraft panels", *Composite Structures*, Vol.71, No. 2, pp.258-270., 2005.

[2] Tong L. and Steven G.P., 1999, *Analysis and Design of Structural Bonded Joints*, Kluwer Academic Publishers, Boston, USA.

[3] Klug J.C. and Sun C.T., 1998, "Large deflection effects of cracked aluminum plates repaired with bonded composite patches", *Composite Structures*, Vol. 42, pp.291-296.

[4] Wang C.H., Rose L.R.F. and Callinan R., 1998, "Analysis of out-of-plane bending in one-sided bonded repair", *International Journal of Solids and Structures*, Vol. 35, pp.1653-1675.

[5] Charalambides, M.N, Kinloch, A.J and Matthews, F.L, "Adhesively-bonded repairs to fibre-composite materials II: finite element modeling", *Composites - Part A: Applied Science and Manufacturing*, Vol. 29, pp.1383-1396, 1998.

[6] Chalkley P. and Baker A., 1999, "Development of a generic repair joint for certification of bonded composite repairs", *International Journal of Adhesion and Adhesives*, Vol. 19, pp.121-132.

[7] Odi, R.A. and Friend C.M, "A comparative study of finite element models for the bonded repair of composite structures", *Journal of Reinforced Plastics and Composites*, Vol. 21, pp.311-332, 2002.

[8] Megueni A, Bachir B.B. and Boutabout B., "Computation of the stress intensity factor for patched crack with bonded composite repair in pure mode II", *Composite Structures*, Vol. 59, pp.415-418, 2003.

[9] Goland M. and Reissner E., 1944, "The stresses in cemented joints", *Journal of Applied Mechanics*, Vol. 11, A17-A27.

[10] Hart-Smith L.J., 1973, *Adhesive-bonded Single-Lap Joints*, CR-112235, NASA Langley Research Center.

[11] Oplinger D.W., 1994, "Effects of adherend deflection on single lap joints", *International Journal of Solids and Structures*, Vol. 31, pp.2565-2587.

[12] Luo Q. and Tong L., 2007, "Fully-coupled nonlinear analysis of single lap adhesive joints", *International Journal of Solids and Structures*, Vol. 44, pp.2349-2370.